MATERIALE PLASTICE
https://revmaterialeplastice.ro
https://doi.org/10.37358/Mat.Plast.1964

Tensile Properties and Manufacturing Defectives of Short Carbon Fiber Specimens Made with the FDM Process

MADALINA-IOANA BLAJ[1*], SEBASTIAN-MARIAN ZAHARIA[1], MIHAI ALIN POP[2], GHEORGHE OANCEA[1]

[1]Transilvania University of Brasov, Technological Engineering and Industrial Management Faculty, Department of Manufacturing Engineering, 5 Mihai Viteazu Str., Brasov, Romania
[2]Transilvania University of Brasov, Material Science and Engineering Faculty, Department of Material Science, 1 Universitatii Str., Brasov, Romania

Abstract: *With the fourth industrial revolution, Additive Manufacturing started to offer new possibilities of manufacturing, Fused Deposition Modeling being one of the most used processes for fabrication. In this paper, the studied specimens are manufactured based on the Fused Deposition Modeling (FDM) method, with a filament of short carbon fiber and polyethylene terephthalate (PET) matrix, with a variation of the layer thickness. For the resulted specimens the tensile properties are determined according to ASTM D638. The most advantageous results are obtained for the layer thickness of 0.15 mm, with the tensile strength of 58 MPa. Based on the stress-strain curves which are presented in this paper, it also can be assumed that the material is brittle. The results of the mechanical properties are very similar for each group of specimens and it can be assumed that the mechanical properties are homogenous due to the material quality and the machine performances. For all the specimens the rupture location is almost in the same area. Due to the difficulty of carbon fiber filament printing, the manufacturing defectives which appear during the manufacturing process are detected, the most common manufacturing defectives being the material gaps from each specimen, which are identified with microstructural analysis. As failure modes, the most common failure criteria are the delamination and the matrix cracks.*

Keywords*: additive manufacturing, fused deposition modeling, short carbon fiber, tensile test*

1. Introduction

Currently, Fused Deposition Modeling (FDM) or Fused Filament Fabrication (FFF) is one of the most used additive manufacturing (AM) processes due to its large number of applications, the involved costs and the production time. As with all the other types of AM processes, the FDM method implies adding in general thermoplastic polymer layer by layer where it is necessary to create a specific part. This technique offers the possibility to create parts with increased complexity in geometry and functionality compared with the conventional manufacturing methods. In general, the used materials have lower values of the mechanical properties and as a result, researchers are oriented to also develop composite filaments to increase them [1].

A composite filament is a mixture of minimum of 2 constituents with different properties, which after merging, the resulting material will have superior characteristics related to each component. The majority of the composite filaments have 2 components: the reinforcing agent, which can be continuous, short or particles and a matrix, which in most cases is a thermoplastic polymer [2]. Common failure criteria noticed for the parts made from composite filaments are registered by delamination or interlaminar failures, matrix cracks, fiber-matrix detachment/debonding, fiber failure or their withdrawal from the matrix. Delamination may appear due to manufacturing reasons: abnormal material deposition cracks between the part layers or matrices with weak mechanical properties, or from mechanical properties with disadvantageous values (residual stresses in interlaminar areas, compression load, or too high loads or fatigue) [1,3].

**email: madalina.blaj@unitbv.ro*

In this paper the focus is on the composite filament with 15% Carbon short fibers/ Chopped carbon-fibers with a polyethylene terephthalate (PET) matrix and their results on tensile tests, failure criteria and manufacturing defectives, with the variation of the layer thickness.

Besides the material used, the mechanical properties are influenced by the 3D printing parameters. The highest influence is offered by the printing direction and the part positioning on the building plate - for tensile, the highest tensile strength is obtained when the part is manufactured in the loading direction, having a similar behavior as the composite materials [4]. Mechanical properties register much lower values in the other directions, because in these directions the material is dependent on the resistance of the matrix and the area between the layers, called interlaminar zone [3] (Figure 1) for its definition.

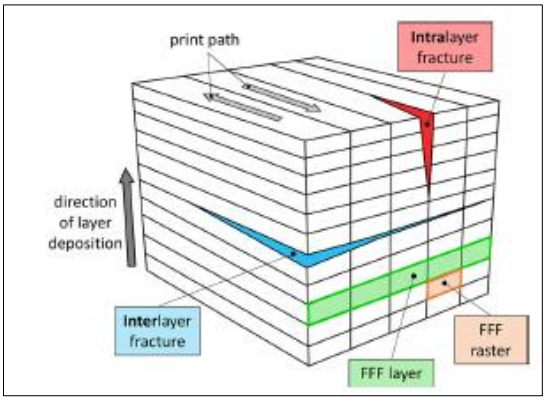

Figure 1. Interlaminar area definition and its defectives [5]

Based on [6], there are 55 design rules developed for FDM and 70% of them are related directly or indirectly to these parameters. Also, the material row direction is an important aspect of the quality of the mechanical properties of the part. If the rows of material overlap completely, then the mechanical properties of the final part will be reduced compared with the situation when the layers are interspersed and the stresses are evenly distributed in all regions of the part [7].

The influence of the thickness layer over the mechanical properties consists in a non-linearity, according to [8], the tensile strength registers a decrease and later an increase in the values once with the increasing value of the layer thickness.

Because this paper focuses on short fibers, according to [9] the fibers increase the strength of the part, but this is reduced by the possibility of the fibers being eliminated from the matrix before their breaking. Also, a comparison is performed with the classical composite materials considering the mechanical properties, these materials have lower performances.

A major influence on the mechanical properties of the short fiber composite filaments results is offered by the porosity of the final part. This manufacturing parameter is influenced by the quantity of fibers - according to [2], it can be seen that the dimensions of the voids tend to have a decrease directly with the increasing quantity of the fibers from the filament. The possibility of distortion of the part is decreased when the quantity of the fibers is increased due to the increased thermal conductivity - increased adhesion of the layers. The material voids can be assumed also to be a weak adhesion between the fibers and the matrix - this depends on the matrix type and also on the material quality.

Besides the mechanical properties advantages, these materials have the possibility of electrical and thermal conductivity and biocompatibility. The references [10, 11] noticed that the length of the fibers during printing suffer modificationsand and those are going to be reduced.

2. Materials and methods

2.1. Machine and material used and manufacturing parameters

The printer used in the research is a BCN3D Sigma, produced by BCN3D Technologies - it can be seen in Figure 2. Its functionality is based on the FDM method, with filament rolls with a diameter of

2.85 mm. The maximum printing dimensions are 210 mm x 297 mm x 210 mm, with a capacity to print up to 50 microns. The diameters of the extrusion heads which can be used range from 0.3 mm up to 1.00 mm. The machine uses 2 extrusion heads [12].

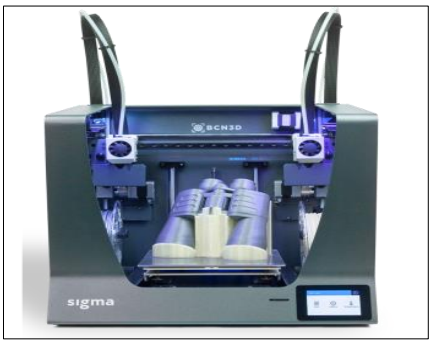

Figure 2. BCN3D Sigma printer [12]

As already mentioned in Section 1, the material used for manufacturing is Innofil (Ultrafuse) PET CF15% with a diameter of 2.85 mm, which is a purchased material [13]. The filament properties can be seen in Table 1.

Table 1. Filament properties [13]

Property	XY Orientation	XZ Orientation	ZX Orientation
Tensile Strength	63.2 MPa	-	12.5 MPa
Elongation at Break	3.7%	-	0.5%
Young Modulus	6178 MPa	-	2822 MPa

During manufacturing, the fan is turned off. The printing parameters are set in BCN3D Cura software program and are described in Table 2.

Table 2. Manufacturing parameters

Parameter	Value
Nozzle Temperature	265°C
Manufacturing Speed	40 mm/s
Platform Temperature	60°C
Layer Thickness	0.15 mm & 0.20 mm
Shell Thickness	1.8 mm
Pattern	Lines

The parts are oriented on the printing platform rotated at 45°, as presented in Figure 3 to obtain the material deposition at 0° and 90°- to maximize the tensile properties.

In total 2 sets of specimens are realized for tensile tests in which only the thickness of the material layer varied: 5 specimens with a thickness of 0.15 mm and 5 specimens with 0.20 mm.

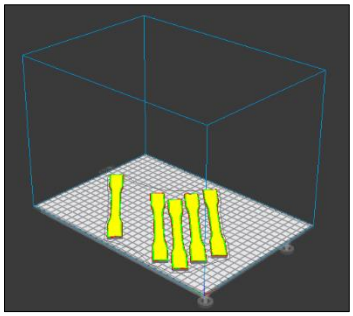

Figure 3. Specimens positioning
on the BCN3D Sigma platform

The specimens are designed according to STM D638 Type I [14] due to the similarity of the printed parts with the composite materials (Figure 4) for the used nominal dimensions - the specimen thickness is 3.2mm.

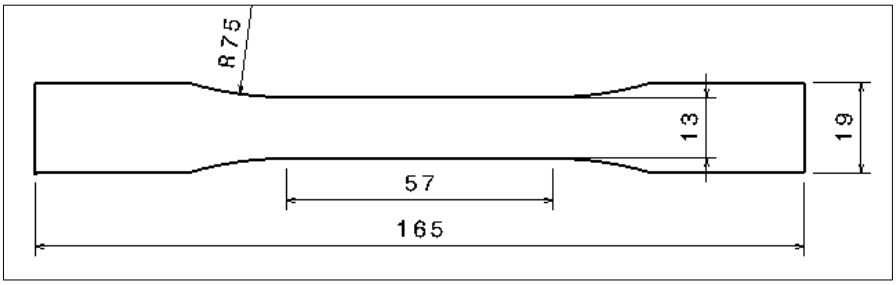

Figure 4. Specimens dimensions according to ASTM D638-14
Type I for Tensile Tests [14]

Even if the specimens are designed to its nominal dimensions, after the manufacturing process the resulted parts have different dimensions. The values are compared with the tolerances range dimensions which are specified in standard and all of them are not exceeding the limits.

The specimens are positioned on the printing platform as presented in Figure 5.

Figure 5. Specimens position
on the printing platform

2.2. Tensile testing machine

The Tensile Testing machine used is a WDW-150S with hydraulic parallel grip and a GW-1200A and YD-350A Controller (Figure 6). The tensile specimens are fixed between the grips as presented in Figure 7.

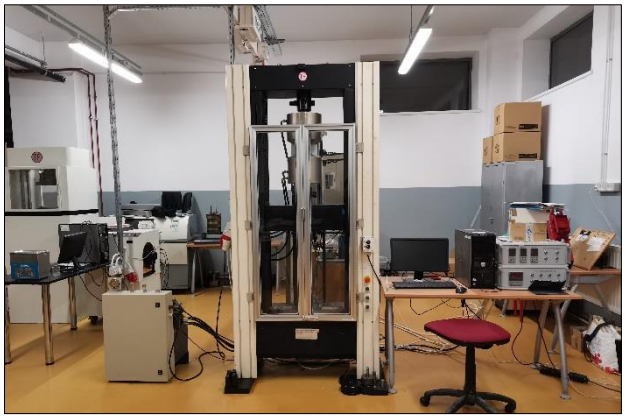

Figure 6. WDW-150S Universal Testing Machine

Figure 7. WDW-150S Superior Electromechanical Universal Testing Machine

The input data for the tensile testing consists of the measurements performed for each specimen, which are introduced in the machine software interface.

2.3. Data post-processing

All the registered data are post-processed to the ASTM D638 Standard [14], removing unwanted outliers for each specimen - the results and discussions are presented in chapter 3.

2.4. Microscopy

After the tests were performed, the specimens are verified with the Nikon T1-SM microscope (Figure 8) to check the microstructure - failure modes and manufacturing issues.

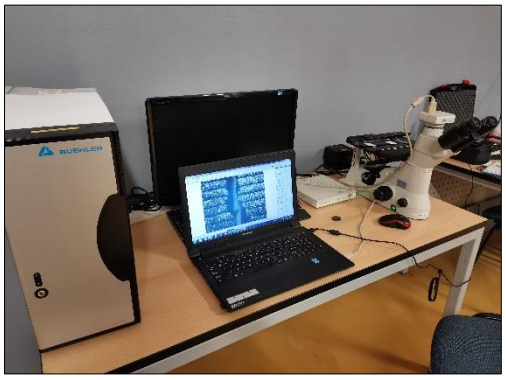

Figure 8. Nikon Eclipse MA 100 Microscope

3. Results and discussions

3.1. Units, abbreviations and, acronyms

σ - Stress (Mpa)
ε - Strain (-)
Fm - Failure Load (kN)
Rm - Tensile Ultimate (Failure) Stress (MPa)
Fp - Yielding Load (kN)
Rp - Tensile Limit (Yield) Strength (MPa)
E - Young Modulus (GPa)

To precisely identify each specimen, a name codification is chosen, as follows:
C_t_I_no, where *t* is the decimals of the layer thickness, *I* is the infill and *no* is the specimen number.

3.2. Results

After the printing, the specimens are visually checked for manufacturing issues (Figure 9) for a specimen after manufacturing - the result is that for each specimen the layers and each material deposition after the nozzle cross can be distinguished. It can be assumed that the material is affected by the decreasing of the temperature gradient after each nozzle pass, causing an incomplete fastening of the material. In Figure 10 it can also be seen that the material deposition is not equally distributed after each cross of the nozzle. This is caused by the nozzle's incapacity to equally distribute the melted material due to a larger amount of fibers into the heated room of the nozzle, which can cause nozzle clogs.

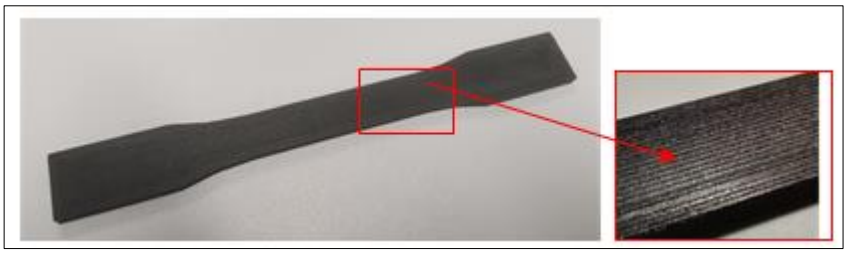

Figure 9. Specimen after manufacturing

After the testing - the specimens can be seen in Figure 11 (left picture - C_15_100; right picture - C_20_100) - and data post-processing, the results are the following:

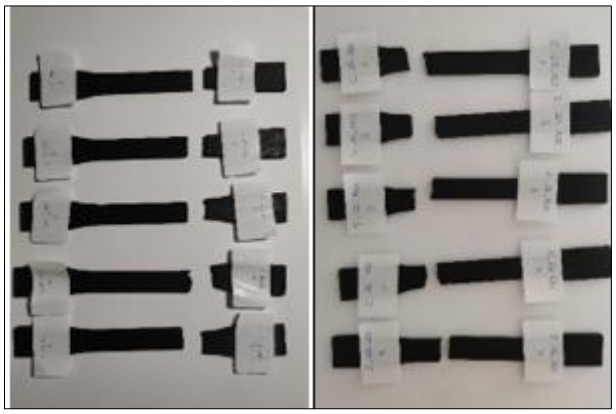

Figure 10. Specimens C_15_100 (Left) and Specimens C_20_100 (Right)

From a macroscopic point of view, the specimens shown in Figure 11 have a similar behavior at tensile rupture, even if the thickness layer is different - the tensile rupture is initiated and continued in almost the

same location and in a same manner for all the specimens. Based on this specimen's behavior, it can be assumed that the filament is qualitative, the carbon fiber quantity being almost equally distributed into the material matrix.

Hereafter, in Figures 11 and 12 the engineering stress-strain curves are presented for each specimen. In Table 2 and Table 3 are presented details regarding the tests, which are also displayed into the stress-strain curves. In the last row of the tables is presented the standard deviation for each parameter considered.

Table 3. Tensile Test results for C_15_100 Specimens

Specimen	Parameter					
	Fm (kN)	Rm (MPa)	Fp (kN)	Rp(kN)	E (GPa)	ε (-)
C_15_100_1	2.431	58	1.477	35	7	1.90
C_15_100_2	2.226	53	1.565	37	6	1.49
C_15_100_3	2.419	58	1.461	35	7	2.19
C_15_100_4	2.449	58	1.481	35	7	1.93
C_15_100_5	2.446	58	1.450	35	7	1.78
Standard deviation	0.094798	2.236067	0.045455	0.894427	0.447213	0.254302

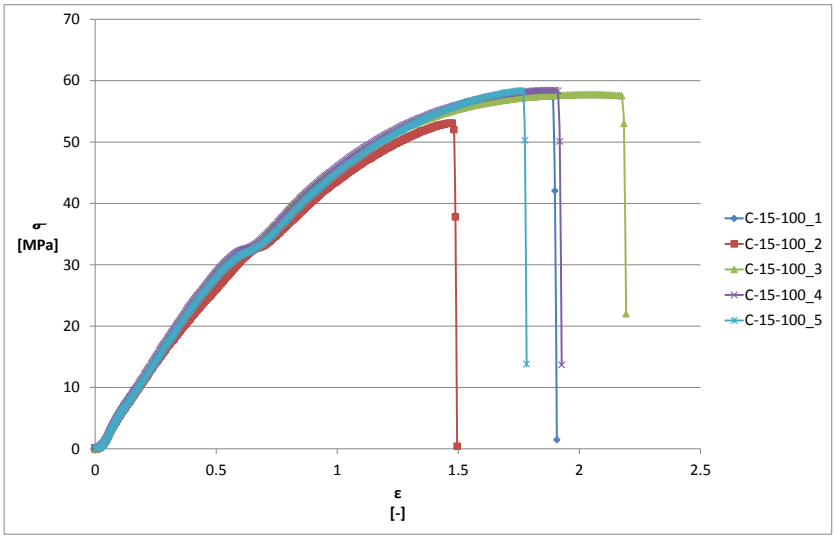

Figure 11. Stress-Strain Curves for C_15_100 1-5 specimens

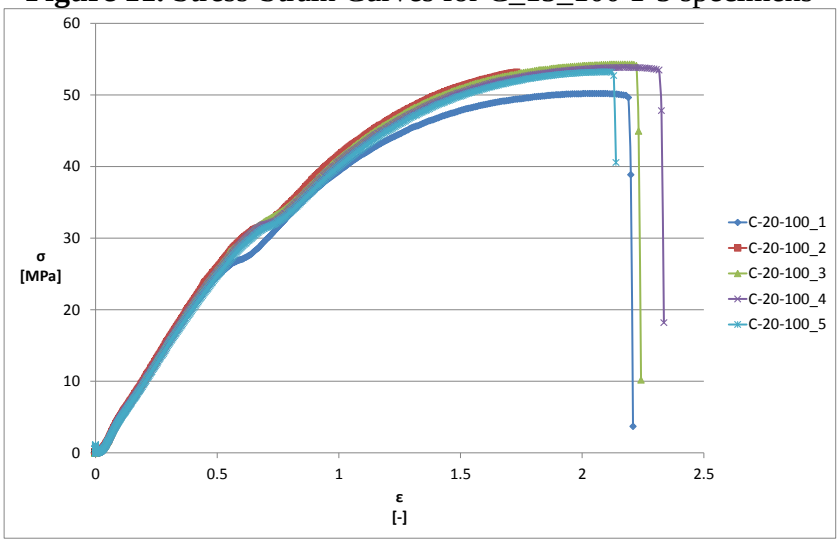

Figure 12. Stress-Strain Curves for C_20_100 1-5 specimens

Table 4. Tensile Test results for C_20_100 Specimens

Specimen	Parameter					
	Fm (kN)	Rm (MPa)	Fp (kN)	Rp(kN)	E (GPa)	ε (-)
C_20_100_1	2.120	50	1.286	30	6	2.20
C_20_100_2	2.297	54	1.398	33	6	2.16
C_20_100_3	2.293	54	1.419	34	6	2.24
C_20_100_4	2.275	54	1.387	33	6	2.34
C_20_100_5	2.248	53	1.383	33	6	2.14
Standard deviation	0.073364	1.732050	0.0514616	1.516575	0	0.079246

Considering the results obtained and presented in Figure 11, Figure 12, Table 2 and Table 3, the specimens have almost the same behavior, except for C_15_100_2, where the largest values difference are registred compared to its homologous. The above tables present the standard deviation for each parameter taken into account with values, compared to each parameter's magnitude level, the deviations are considered to be acceptable in order to view the material as homogenous on its mechanical properties. Even so, comparing the mechanical properties results based on the thickness layer, the most homogenous and advantageous results are obtained for the specimens with a layer thickness of 0.15 mm, if the most important parameters are σ and E. Similar results are obtained also in [15], where the lower value of the thickness layer registered better tensile properties. Otherwise if the comparison is performed considering the elongation, the highest values are recorded for the thickness layer of 0.20 mm. The tensile strength values are lower compared with the same filament properties values for XY orientation presented in Table 1.

For the specimens C_15_100, the failure and yield strength values are the same (excluding the exception registered in C_15_100_2), the difference being made by the elongation registered for each specimen - the maximum value is 2.19 and the lowest value being 1.78, which means a difference of 23%, which is lower compared with the values from Table 1 from XY orientation. Calculating an average between the considered values, the strain can be considered 1.95. The Young Modulus is 7 GPa, which is a higher value compared with the filament properties described in Table 1.

For the specimens C_20_100, the failure and yield strength have almost the same values. In this case, there are no large differences between the elongation values, the difference between the minimum value and the maximum value is 9.34%.

The homogeneity of the results can be assigned to the machine capacity to maintain the temperature into the nozzle and also the bed temperature as well as to the filament quality (the diameter of the filament has lower-dimensional tolerances and the carbon fibers are distributed almost equally in the matrix).

Based on Figure 10 - which shows the specimens ruptures with no visible neckings and the stress-strain results - higher strength and lower elongation, the material is considered to be brittle.

Hereafter, Figure 13 shows the failure area of C_15_100_1 and also the delimitations of the rasters. The carbon fibers can also be seen, which due to the failure, did not break, but they came out of the matrix. Figure 14 shows the carbon fibers orientation that is not in the printing direction as [10, 16, 17] state. Also, a manufacturing issue is visible, a material conglomerate. This affects the material deposition, the raster's alignment and the linearity.

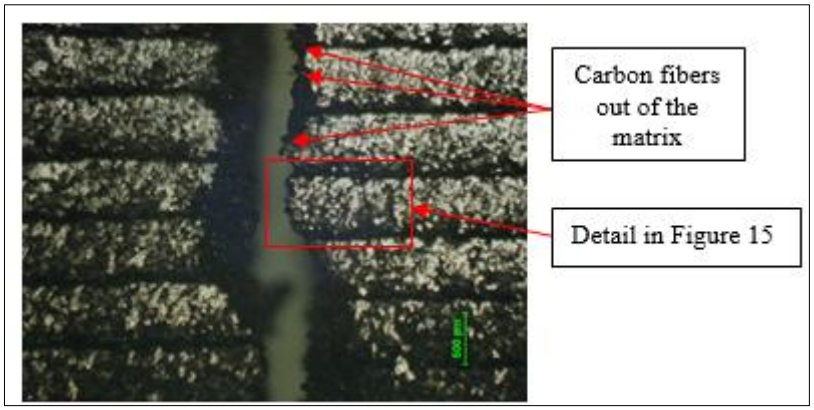

Figure 13. Microscope image x25 zoom in - C_15_100_1 - Failure area - Top view

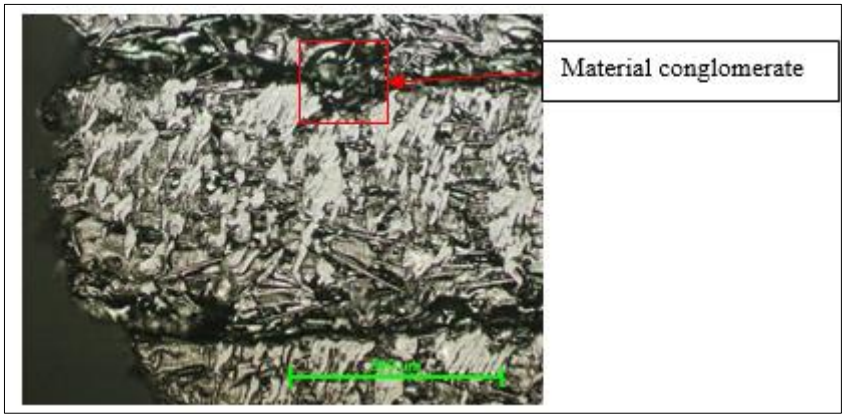

Figure 14. Microscope image x100 zoom in - C_15_100_1 - Failure area - Top view

Figure 15 shows the failure area of C_20_100_5 and also the joining area between the shell and the layers. The view is blurred in some areas due to irregular rupture during the tensile test. A multitude of material gaps can also be seen - only several gaps are highlighted - it can be assumed that the PET does not adhere to the carbon fibers. This issue affects the mechanical properties. After checking all the specimens, the gaps appear in all of them, also as is stated in [15, 17]. Figure 15 shows the delimitation between the 0° and 90° oriented layers.

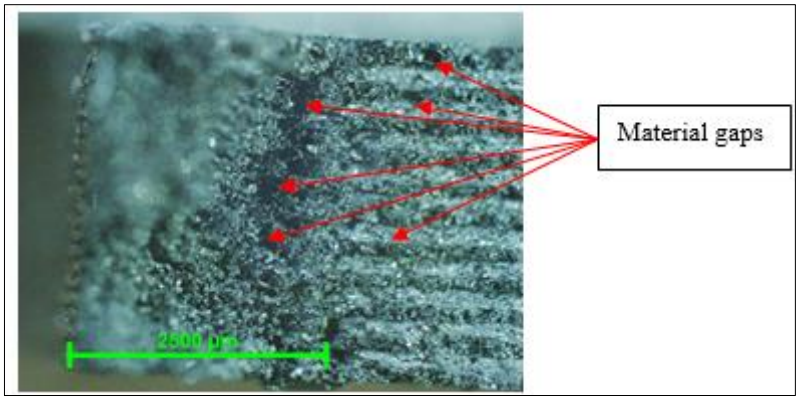

Figure 15. Microscope image x25 zoom in - C_20_100_5 - Failure area - Lateral view

Hereafter, Figure 16 are presented the failure area of C_15_100_3 where delamination occurs and also a crack appears and propagates between the layers. In Figure 16 material gaps are presented

Hereafter, in Figure 16 are presented the failure area of C_15_100_3 where delamination occurs and also a crack appears and propagates between the layers. In Figure 16 material gaps are presented.

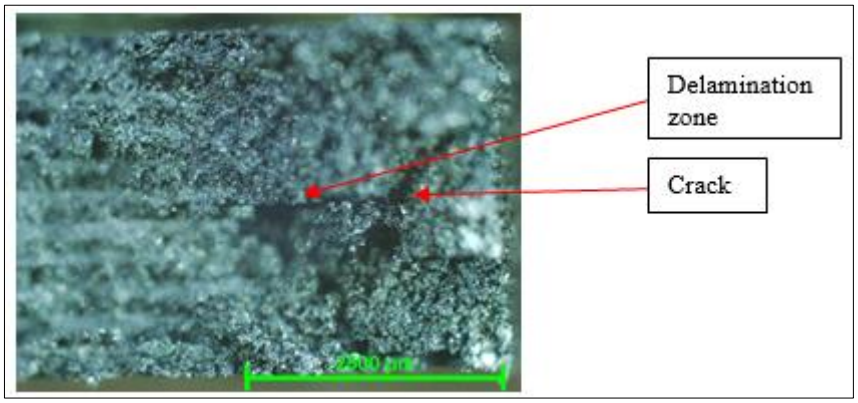

Figure 16. Microscope image x25 zoom
in - C_20_100_3 - Failure area - Lateral view

4. Conclusions

All in all it can be stated that the behavior of the carbon fiber filament with PET matrix is brittle. The mechanical properties are homogenous due to the material quality and the machine performance. Considering the layer thickness, the most advantageous results are obtained for the layer thickness of 0.15 mm for the strength and Young Modulus and the thickness layer of 0.20 mm for elongation.

As failure modes, the rupture is similar for all the specimens. Cracks in other directions can also appear, and also layers delamination. During rupture, the carbon fibers can come out of the matrix and also due to PET matrix does not adhere to the carbon fibers, material gaps appear in all the manufactured parts.

Another manufacturing defect is the gap between the layers and the rasters due to a fast decrease of the deposited material temperature gradient. It appears in all of the parts, affecting the mechanical behavior of the specimens. Due to the possibility of defective filament, the material conglomerate can appear, affecting the linearity and the dimensions of the rasters/ layers.

Based on the fact that the fibers are not aligned on the manufacturing direction and also due to the rasters and layers orientations, the material is considered to be anisotropic. In further research, a FEM analysis will be performed with the hypothesis of a composite material with short fibers and with a default orientation.

References

1. BLAJ, M., OANCEA, GH., Fused deposition modeling process: a literature review, **1009**, 2021
2. GOH, G.D., DIKSHIT, V., NAGALINGAM, A.P., GOH, G.L., AGARWALA, S., SING, S.L., WEI, J., YEONG, W.Y., Characterization of mechanical properties and fracture mode of additively manufactured carbon fiber and glass fiber reinforced thermoplastics, **137**, 2018, 79-89
3.D'AMICO, A., PETERSON, A.M., An adaptable FEA simulation of material extrusion additive manufacturing heat transfer in 3D, **21**, 2018, 422-430
4. CHACÓN, J.M., CAMINERO, M.A., GARCÍA-PLAZA, E., NÚÑEZ, P.J., Additive manufacturing of PLA structures using fused deposition modelling: Effect of process parameters on mechanical properties and their optimal selection, **124**, 2017, 143-157
5.YOUNG, D., WETMORE, N., CZABAJ, M., Interlayer fracture toughness of additively manufactured unreinforced and carbon-fiber-reinforced acrylonitrile butadiene styrene, **22**, 2018, 508-515
6. LEUTENECKER-TWELSIEK, B., KLAHN, C., MEBOLDT, M., Considering Part Orientation in Design for Additive Manufacturing, **50**, 2016, 408-413

7. GIBSON, I., ROSEN, D., STUCKER, B., *Additive Manufacturing Technologies – 3D Printing, Rapid Prototyping, and Direct Digital Manufacturing, Second Edition*, Springer, New York, 2015
8.O'CONNOR, H. J., DOWLING, D. P., Evaluation of the influence of low pressure additive manufacturing processing conditions on printed polymer parts, **21**, 2018, 404-412
9.VANEKER, T. H. J., Material extrusion of continuous fiber reinforced plastics using commingled yarn, **66**, 2017, 317-322
10. JIANG, D., SMITH, D. E., Anisotropic mechanical properties of oriented carbon fiber filled polymer composites produced with fused filament fabrication, **18**, 2017, 84-94
11. BLOK, L. G., LONGANA, M. L., YU, H., WOODS, B. K. S., An investigation into 3D printing of fibre reinforced thermoplastic composites, **22**, 2018, 176-186
12.***https://www.filamente3d.ro/imprimante-3d/imprimanta-bcn3d-sigma (accessed on 07.03.2021)
13.***https://www.ultrafusefff.com/product/ultrafuse-pet-cf-black-2-85mm-750g / (accessed on 07.03. 2021)
14. ***ASTM D638-14 Standard
15. SOMIREDDY, M., SINGH, C.V., CZEKANSKI, A., Mechanical behaviour of 3D printed composite parts with short carbon fiber reinforcements, **107**, 2019, 104232
16.SOMIREDDY, M., CZEKANSKI, A., Anisotropic material behaviour of 3D printed composite structures - Material extrusion additive manufacturing, **195**, 2020, 108953
17. SCAPIN, M., PERONI, L., Numerical Simulations of Components Produced by Fused Deposition 3D Printing, **14**, 2021, 4625

Manuscript received: 28.10.2021